ELSEVIER

Available online at www.sciencedirect.com
SCIENCE DIRECT®

Ultramicroscopy 102 (2004) 51–59

ultramicroscopy

www.elsevier.com/locate/ultramic

Influence of the atomic force microscope tip on the multifractal analysis of rough surfaces

Petr Klapetek[a,b,*], Ivan Ohlídal[b], Jindřich Bílek[b]

[a]Czech Metrology Institute, Okružní 31, 638 00 Brno, Czech Republic
[b]Department of Physical Electronics, Faculty of Science, Masaryk University, Kotlářská 2, 611 37 Brno, Czech Republic

Received 17 February 2004; received in revised form 9 August 2004; accepted 20 August 2004

Abstract

In this paper, the influence of atomic force microscope tip on the multifractal analysis of rough surfaces is discussed. This analysis is based on two methods, i.e. on the correlation function method and the wavelet transform modulus maxima method. The principles of both methods are briefly described. Both methods are applied to simulated rough surfaces (simulation is performed by the spectral synthesis method). It is shown that the finite dimensions of the microscope tip misrepresent the values of the quantities expressing the multifractal analysis of rough surfaces within both the methods. Thus, it was concretely shown that the influence of the finite dimensions of the microscope tip changed mono-fractal properties of simulated rough surface to multifractal ones. Further, it is shown that a surface reconstruction method developed for removing the negative influence of the microscope tip does not improve the results obtained in a substantial way. The theoretical procedures concerning both the methods, i.e. the correlation function method and the wavelet transform modulus maxima method, are illustrated for the multifractal analysis of randomly rough gallium arsenide surfaces prepared by means of the thermal oxidation of smooth gallium arsenide surfaces and subsequent dissolution of the oxide films.
© 2004 Elsevier B.V. All rights reserved.

PACS: 61.16.Ch; 61.43.Hv

Keywords: Roughness; AFM

1. Introduction

In general, fractals are objects having identical geometrical properties even after magnification and change of scale. These fractals are classified into two groups. The first group is formed by self-similar fractals. Self-similar fractals exhibit the same geometrical properties after isotropic magnification and change of scale. Self-affine fractals differ from self-similar ones in such a way that the magnification is anisotropic, i.e. this magnification

*Corresponding author.
E-mail address: klapetek@physics.muni.cz (P. Klapetek).

0304-3991/$ - see front matter © 2004 Elsevier B.V. All rights reserved.
doi:10.1016/j.ultramic.2004.08.005

is different in different directions. Random fractals exhibit similar properties from the point of view of their statistical properties. Therefore, the magnified and rescaled random fractals are not exactly identical to the original ones. Only the statistical properties of these fractals are identical to the statistical properties of the original fractals, i.e. the fractals without magnification.

In practice, objects exhibiting random properties are encountered. It is often assumed that these objects exhibit self-affine properties in a certain range of scales. Many randomly rough surfaces belong to the random objects that exhibit self-affine properties. These surfaces can be studied using atomic force microscopy (AFM). The results of fractal analysis of self-affine random surfaces by AFM are often used to classify surfaces prepared by various technological procedures [1–4].

However, it is known that the values of quantities characterizing randomly rough surfaces determined using AFM are frequently influenced by a process of measurement. These results are mainly influenced by finite dimensions of the tip of the atomic force microscope. In this paper the influence of the tip on the multifractal properties will therefore be studied. It should be noted that the influence of AFM measurements on the results of the fractal analysis was partially investigated in several papers [5,6]. In these papers it was shown that it could be very problematic to compare results of the fractal analysis of the surfaces obtained by different analytical methods. Therefore, we will employ the multifractal analysis for studying AFM tip influence on the fractal properties of randomly rough surfaces. In contrast to the fractal analysis the multifractal method is more complex. This multifractal analysis enables us to determine more parameters characterizing random surfaces.

For analyzing the tip influence on the multifractal properties of AFM data, we will simulate and analyze surfaces with known fractal properties, we will perform virtual "tip convolution" and we will analyze surfaces again. To analyze possibilities of removing tip influence from the data we will further perform surface reconstruction and analyze reconstructed data.

Two methods of multifractal analysis will be used. The first one is called the correlation function (CF) method employed for the fractal analysis using AFM in Ref. [7]. The second method is called the wavelet transform modulus maxima (WTMM) method. The WTMM method is new and to our knowledge it has not been employed within AFM analysis of rough surfaces so far. The results achieved using both analytical methods will be compared.

2. Analysis of the multifractal properties of rough surfaces

The CF method is based on the measurement of the one-dimensional correlation function defined as follows:

$$G_{x,q}(\tau_x) = \frac{1}{N(M-m)} \sum_{l=1}^{N} \sum_{n=1}^{M-m} |z_{n+m,l} - z_{n,l}|^q, \qquad (1)$$

where $m = \tau_x/\Delta$, $N \times M$ is scan size (N and M denote the numbers of rows and columns in the scan), $z_{n,l}$ and $z_{n+m,l}$ represent the values of the heights of the irregularities of the surface in two different points of this surface, τ_x is the distance between the points with the heights $z_{n,l}$ and $z_{n+m,l}$, Δ is the sampling interval and q is the order of the correlation function. Note that the one-dimensional correlation function is only determined along the rows of the scan.

Below, it will be assumed that the scaling behavior of the function $G_{x,q}$ is given as

$$G_{x,q}(\tau_x) \sim \tau_x^{qH_q}, \qquad (2)$$

where H_q denote the Hurst exponent corresponding to a given order of the correlation function. If all the coefficients H_q are equal, Eq. (2) describes a self-affine surface with monofractal properties. If the coefficients H_q are different for at least some values of order q we talk about surface having multifractal properties. Such the surfaces can be described by a set of the values of H_q.

The WTMM method is based on the ability of the continuous wavelet transform to detect singularities. Wavelet transform of the one-dimensional signal $f(x)$ is defined as

$$W[f](a,b) = \frac{1}{\sqrt{|a|}} \int_{-\infty}^{\infty} f(x)\phi^*\left(\frac{(x-b)}{a}\right) \mathrm{d}x, \qquad (3)$$

where function $\phi(x)$ is called the wavelet, parameter a controls the scale of the wavelet (its magnification) and parameter b controls its shift along the time axis. Wavelet transform decomposes the signal into space-frequency domain in a way similar to the windowed (short-time) Fourier transform. However, in contrary to the windowed Fourier transform, the spatial resolution of different frequency components is not the same, but depends on the frequency of the component (determined by corresponding scale parameter). When going towards smaller scales, the wavelet transform of a signal shows more and more details of the signal. Therefore, it is sometimes called as a "mathematical microscope" [8]. It can be shown that these properties of the wavelet transform can be efficiently used for determining properties of singularities in the signal [8].

Within the one-dimensional WTMM method (see e.g. Refs. [8,9]), a continuous wavelet transform of the function $f(x)$ is calculated for a finite number of scales $(a_{\min}, \ldots, a_{\max})$ using the derivative of Gaussian wavelet usually. The local maxima of the wavelet transform modulus for each scale is found. Then the nearest-neighbor maxima between the adjacent scales are connected from the smallest scale $a_{\min}$ up to largest scale $a_{\max}$. In this way maxima lines are created. From the dependence of wavelet transform modulus maxima values on corresponding scales the Hölder exponent of the singularities present at the signal $f(x)$ is obtained. The power law proportionality for the wavelet transform of the signal $W[f](a, x_0)$ is then expected to be

$$|W[f](a, x_0)| \sim a^{h(x_0)} \tag{4}$$

for the maxima line pointing to the singularity x_0 at the lower scale limit. From the log–log plot of the WTMM values corresponding to maxima lines versus the scales the Hölder exponent at x_0 can be evaluated.

The above-mentioned approach to the singularity detection and its strength evaluation can be extended into two dimensions as was done by Arneodo [10] or to even more dimensions. The two-dimensional procedure described in Ref. [10] is very similar to the one-dimensional one.

A two-dimensional continuous wavelet transform with the Gaussian wavelet given as $\phi(\mathbf{r}) = \exp(-\mathbf{r}^2/2)$ is performed corresponding to its definition as

$$T_\phi[f](\mathbf{b}, a) = a^{-2} \iint \mathrm{d}^2\mathbf{r}\, \phi((\mathbf{r} - \mathbf{b})/a) f(\mathbf{r}). \tag{5}$$

Then the vector $\mathbf{T}_\psi$ is constructed as

$$\mathbf{T}_\psi[f](\mathbf{b}, a) = \nabla\{T_\phi[f](\mathbf{b}, a)\}. \tag{6}$$

The wavelet transform modulus maxima are then evaluated using the modulus $\mathcal{M}_\psi[f](\mathbf{b}, a)$ and argument $\mathcal{A}_\psi[f](\mathbf{b}, a)$ of the vector $\mathbf{T}_\psi[f](\mathbf{b}, a)$. Note that in fact the vector $\mathbf{T}_\psi[f]$ corresponds to a wavelet transform using two wavelets, ψ_1 and ψ_2, each one formed by derivation of the Gaussian wavelet in x or y direction, respectively. The wavelet transform modulus maxima (WTMM) are defined at the positions where the modulus $\mathcal{M}_\psi[f](\mathbf{b}, a)$ is locally maximum in the direction $\mathcal{A}_\psi[f](\mathbf{b}, a)$ of the gradient vector $\mathbf{T}_\psi[f]$. For rough surfaces, these local maxima lie on connected chains (see Fig. 7). The WTMM maxima (WTMMM) are then identified as local maxima of $\mathcal{M}_\psi[f](\mathbf{b}, a)$ along these connected chains. The WTMMM are finally connected between the scales forming a set of the maxima lines $\{\mathcal{L}\}$. The whole set of maxima lines is called wavelet transform skeleton (see Fig. 8). In the case of isolated singularities, the Hölder exponents corresponding to the singularities can be obtained in the same way as for one-dimensional signals [8] from the maxima lines.

However, the above-mentioned approach cannot be used in the case when the singularities are not isolated, as in the case of the time series (one-dimensional) or surfaces (two-dimensional) with random character. In this case a scale-adaptive partition function [10] must be used as

$$\mathcal{Z}(q, a) = \sum_{\mathcal{L} \in \mathcal{L}(a)} \left(\sup_{(\mathbf{x}, a') \in \mathcal{L}, a' \leqslant a} \mathcal{M}_\psi[f](\mathbf{x}, a') \right)^q, \tag{7}$$

where q is the order of the partition function. The contributions for each scale of the maxima lines still present at that scale are thus summed. Scaling exponent $\tau(q)$ is defined by means of relation

$$\mathcal{Z}(q, a) \sim a^{\tau(q)}. \tag{8}$$

From this scaling exponent the singularity spectrum $D(h)$ can further be calculated as its Legendre transform $D(h) = \min_q(qh - \tau(q))$. This spectrum is defined as the Hausdorff dimension of the set of points where the Hölder exponent of f is h. From the statistical point of view it is important to determine the function $\mathscr{Z}(q,a)$ from a large wavelet skeleton. As the images have usually limited size in practice, and moreover, we want to evaluate more realizations of the stochastic process, it is necessary to use averaging in the computation of $\mathscr{Z}(q,a)$ as it is proposed in Ref. [10].

The fractal dimension of the surface can be evaluated from the scaling exponent $\tau(1)$ as

$$D_{\rm f} = \max(2, 1 - \tau(1)). \quad (9)$$

Moreover, it can be shown that for fractional Brownian surfaces, the $\tau(q)$ scaling exponents are also connected with the Hurst exponent H of the surface as [10]

$$\tau(q) = qH - 2, \quad (10)$$

i.e. the $\tau(q)$ function is a linear function of q with slope given by H. The linearity of the function $\tau(q)$ is thus a sign of monofractal properties of the surface. Moreover, from the dependences of $\tau(q)$ it is possible to determine the Hurst exponent of the surface.

3. Tip influence on results of multifractal analysis

It is known that some artifacts (systematic errors) arise in AFM measurements of all fine structures. The main artifact concerns the "tip convolution" due to the fact that the tip exhibits finite linear dimensions (i.e. the tip has not an ideal form represented by the δ-function). This effect causes a misrepresentation of the data describing a fine surface geometry studied. Here we shall deal with the theoretical analysis concerning the influence of the tip dimensions on the values of the multifractal properties characterizing the surface roughness based on the following stages:

(1) The self-affine surface structure is simulated by means of spectral synthesis method (see below). Further, the fractal properties of this simulated surface are determined.
(2) Using the algorithm presented by Villarubia's algorithm [11] an AFM image of the simulated surface is simulated for a chosen AFM tip geometry.
(3) The multifractal properties are determined using the data corresponding to this image, i.e. using the data corresponding to the structure influenced by the tip dimensions (uncorrected structure).
(4) Using the surface reconstruction developed by Villarubia [11] the tip effect on the surface is partially corrected.
(5) The multifractal properties corresponding to the corrected surface are determined.

For this purpose procedures presented by Villarubia were employed in this paper. The first Villarubia's procedure (tip–sample dilation) enables us to include the influence of the finite dimensions of the tip on the geometry of the surface measured, i.e. it enables us to construct the surface measured using a AFM tip. The second Villarubia's procedure (erosion) enables us to perform a correction of the measured (misrepresented) surface. A schematic diagram showing the surface profiles obtained using the Villarubia's procedures is introduced in Fig. 1.

For the purposes of our theoretical analysis we chose a model of the standard pyramidal contact AFM tip (i.e. this tip was formed by a pyramid

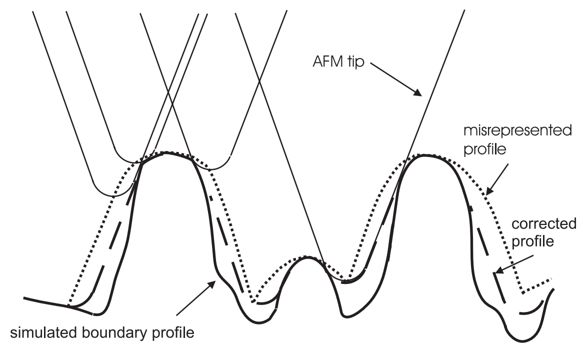

Fig. 1. Schematic diagram expressing the influence of the tip on measuring the profile of the rough surface and improvement of this profile measured using the correcting procedure employed.

with a spherical apex). The apex radius was equal to 10 nm. This corresponds to a real contact or noncontact tip properties.

4. Preparation of samples and experimental arrangement

The surfaces of the GaAs (1 0 0)-oriented n-type single-crystal wafers were polished and etched in the standard way. Using AFM it was found that the values of the RMS value of heights of these surfaces were smaller than 0.5 nm, i.e. these GaAs surfaces can be considered to be smooth from the practical point of view. The smooth GaAs wafers were then oxidized in air at temperature 500 °C in a tube furnace. The fluctuation in temperature during oxidation did not exceed ±0.5 °C. The oxide layers grown on the GaAs surfaces were dissolved in a mixture of hydrofluoric acid and water and the samples obtained were studied experimentally. Note that before dissolving the oxide layers their upper boundaries were studied using AFM as well. The time of oxidation was 8 h.

For analyzing the GaAs surfaces the commercial apparatus, ThermoMicroscopes Explorer, was used. Both contact and noncontact modes were used for the measurements. Both the standard contact (apex ratio 1 : 2, apex curvature <20 nm) and noncontact (apex ratio 1 : 10, apex curvature <10 nm) tips were utilized.

5. Results and discussion

For simulation of the surfaces with well-defined multifractal properties a spectral synthesis method (see e.g. Ref. [12]) is used. This method is designed to produce surfaces with the properties of the fractional Brownian surfaces. Fractional Brownian motion (fBm) is an extension of regular Brownian random walk for which the correlation between successive steps is controlled by a parameter H known as the Hurst exponent. The Hurst exponent defines a scaling relation [12]

$$E[(X_t - X_{t'})^2] \propto (t - t')^{2H}, \qquad (11)$$

where $E[(X_t - X_{t'})^2]$ is the expected variance of successive increments, X_t and $X_{t'}$, of the random walk spaced a distance $t - t'$ apart.

The spectral synthesis method enables us to define the required Hurst exponent H of the surface (measure of regularity) that is connected with the fractal dimension D_{f} of the surface as $D = 3 - H$.

We have tested both the CF method and the WTMM method on sets of isotropic fractional Brownian surfaces generated by the spectral synthesis method. We used a set of 25 images (1024×1024) for each fractal dimension within the interval $(2.1, 2.2, \ldots, 2.9)$ and we averaged the results of these images.

Correlation functions of different order q were calculated using Eq. (1). In Fig. 2a the dependences of resulting values H_q on q are plotted for generated surfaces with different fractal dimensions. We can see that these dependences are constant. Finally, in Fig. 2b the resulting fractal dimensions are plotted versus the nominal ones (used for the generation of fBm surfaces).

Note that the discrepancies between ideal results (shown as the dotted line) and real results are given by both the processes, i.e. generation of the surface and evaluation of its properties.

The same analysis was performed for the WTMM method. In Fig. 3a, the dependences of $\tau(q)$ are plotted for fBm surfaces generated at different Hurst exponents. We can see that these dependences have a linear form as expected for the fBm surfaces. In Fig. 3b, the dependence between a generating fractal dimension and a fractal dimension determined by means of the WTMM is plotted.

Note that, in Ref. [10] even a larger set is proposed to be used to obtain the right values of the fractal dimension for the generated fractional Brownian surfaces. However, within AFM measurements, it is rather complicated (time consuming) to obtain really large sets of images for one surface. In practice, while evaluating the statistical properties of rough surfaces we usually work with five or ten AFM images for each surface.

The surfaces having nominal fractal dimension of 2.5 were then scaled to have dimensions typical for the real applications. These surfaces were

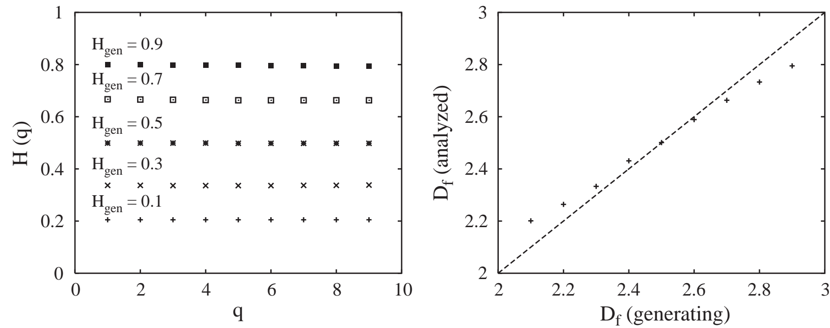

Fig. 2. qth-order correlation function results: left—parameters H_q for generating Hurst exponents of 0.1, 0.3, 0.5, 0.7 and 0.9. right—generating vs. analyzed fractal dimension for fBm rough surfaces.

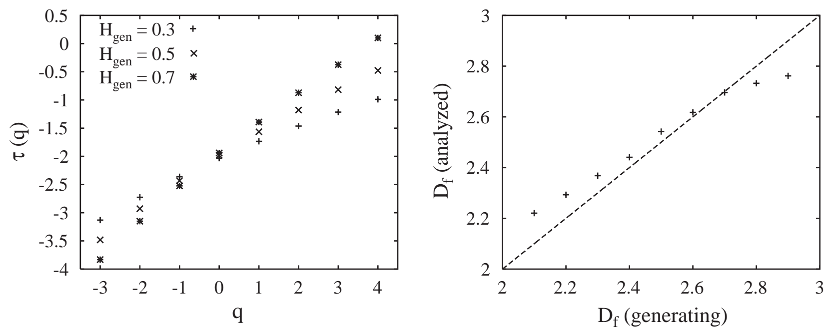

Fig. 3. (left)-dependences of $\tau(q)$ for fBm surfaces with $H = 0.3$, 0.5 and 0.7, (right)-dependence between generating fractal dimension and fractal dimension determined by means of the WTMM.

dilated to take into account the finite AFM tip apex sizes (misrepresented data) and then these surfaces were reconstructed to obtain the corrected surfaces. For the analysis we used four different tip radii 20, 50, 70 and 100 nm. Images of the surfaces after dilation can be seen in Fig. 4.

The results concerning multifractal analysis of the simulated, misrepresented and corrected surfaces are shown in Figs. 5 and 6. These results were obtained using both the methods used for the multifractal properties study—correlation function method and wavelet transform modulus maxima method. In Fig. 5 is seen that for both methods the results obtained for analysis of misrepresented surfaces exhibit similar properties. First of all, the value of the fractal dimension evaluated using the assumption of monofractal surface is decreasing (the values of $H(2)$ and $\tau(1)$ are increasing). Moreover, the shapes of the $H(q)$ and $\tau(q)$ differ from their linear character and the surfaces tend to exhibit multifractal properties.

Similar results can be shown also for corrected surfaces (see Fig. 6). Here the same effect can be observed as for the misrepresented surfaces. Thus, it can be seen that the correction procedure (surface reconstruction) has not desired the effect from the point of view of the fractal properties.

Finally, we applied the WTMM method on the GaAs surfaces created by thermal oxidation and dissolution of the oxide layer. In Fig. 7, the WTMM maxima for two different scales are plotted. The local maxima within the closed maxima chains are marked by crosses. In Fig. 8, the wavelet transform skeleton of GaAs sample corresponding to the time of oxidation of 8 h is presented.

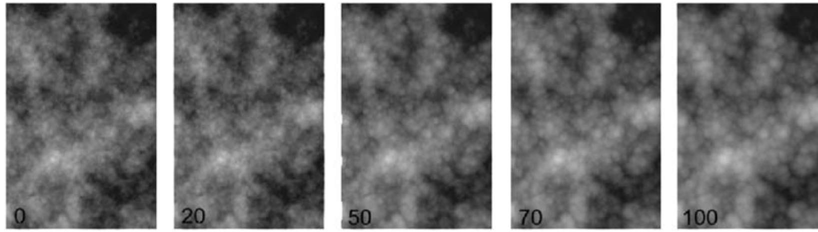

Fig. 4. Images of the simulated fractional Brownian surfaces with dilations (tip convolutions) applied: (from the left) no dilation, after dilation with tip having apex radius of 20, 50, 70 and 100 nm.

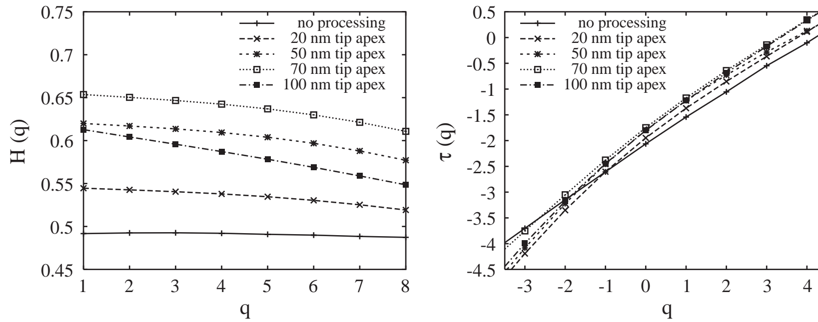

Fig. 5. Fractal surface properties after dilation using simulated AFM tip with different apex radii: left—correlation function results, right—WTMM results.

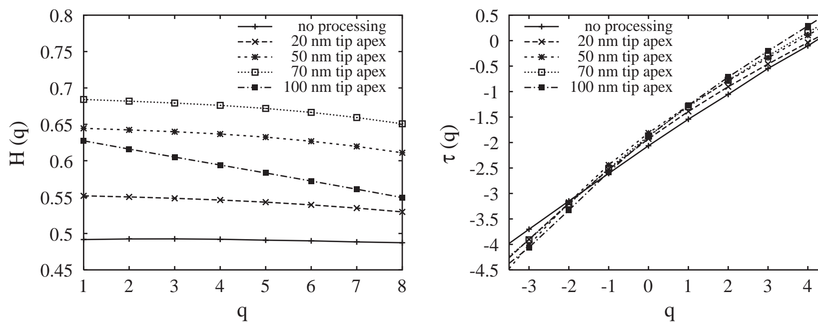

Fig. 6. Fractal surface properties after dilation and reconstruction (for dilated surface properties see Fig. 5): left—correlation function results, right—the WTMM results.

Within the height–height correlation function method and the WTMM method it was found that the fractal dimensions of GaAs surfaces created by thermal oxidation and dissolution of the oxide layer were typically within the interval (2.4 ± 0.1). Moreover, the dependence of $\tau(q)$ on q was not strictly linear as given by Eq. (10) for the real surfaces (see Fig. 9). In principle, this is a sign of multifractal properties. However, a much larger set of AFM images would be necessary for each sample to study the multifractality in a quantitative way. However, in practice it can be rather complicated and time consuming to obtain really large data sets of AFM samples (around 30 images of each sample). Moreover, the nonlinearity of the corresponding functions can be also caused by the tip convolution effects as discussed above. In principle, these effects can be hardly separated

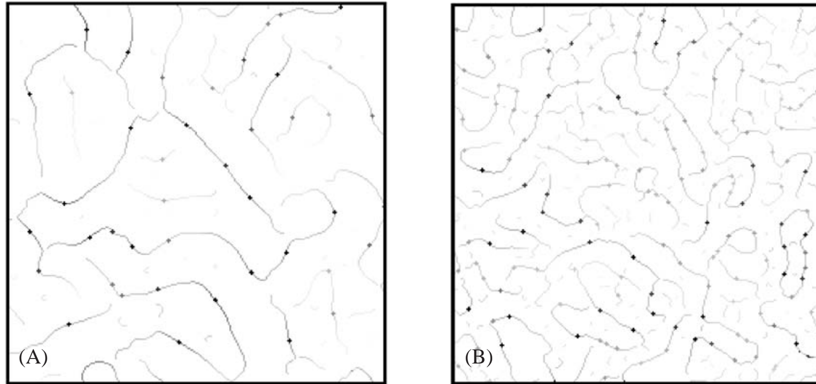

Fig. 7. The WTMM maxima lying on a connected chains for two different scales (A—higher scale, B—smaller scale). The local maxima within these chains are marked by crosses. This images were obtained while analyzing the GaAs sample corresponding to the time of oxidation of 8 h.

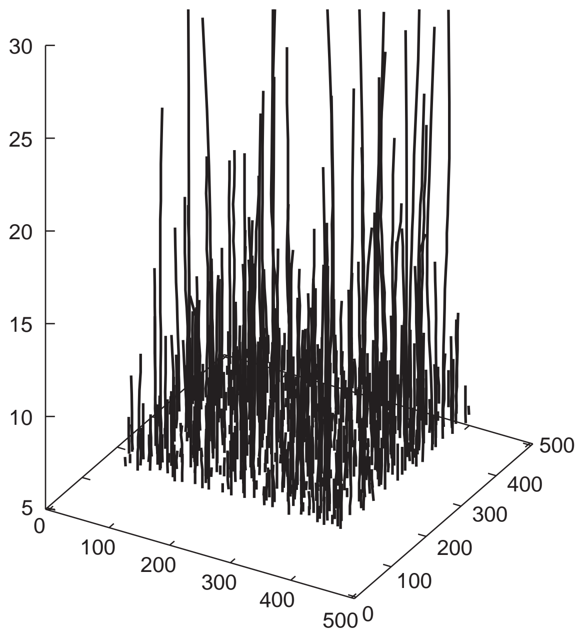

Fig. 8. Wavelet transform skeleton of GaAs sample corresponding to the time of oxidation of 8 h.

from the results, namely from results obtained on samples having real sizes of objects forming roughness similar to AFM tip apex size.

If we compare the results of both the multifractal analysis methods used in this article while analyzing generated fractal surfaces (Figs. 1b and 2b), we can see that principally there is no considerable difference in their results. Note that the errors observed for very small and very high values of fractal dimension are more or less typical for all the fractal analysis methods. It can be also seen that the presumption of linearity of H_q spectrum (CF method) and $\tau(q)$ spectrum (WTMM) for monofractal data is valid for both methods too. From this point of view both methods are comparable.

However, from the point of real data analysis in practical applications we should note that the WTMM method is significantly slower than the CF method from the point of view of computations. Moreover, the WTMM method is much more sensitive to sharp discontinuities on the surface related to random errors that can be present in AFM scan than the CF method. Therefore, high quality AFM images must be used to perform the WTMM analysis.

6. Conclusion

Theoretical analysis of multifractal properties of the randomly rough surfaces was performed. It was shown that the tip convolution effects could change the estimated value of fractal dimension. Moreover, they can also introduce a nonlinearity into the multifractal spectra that is not present in the original surface. This fact should therefore be respected when interpreting the results concerning

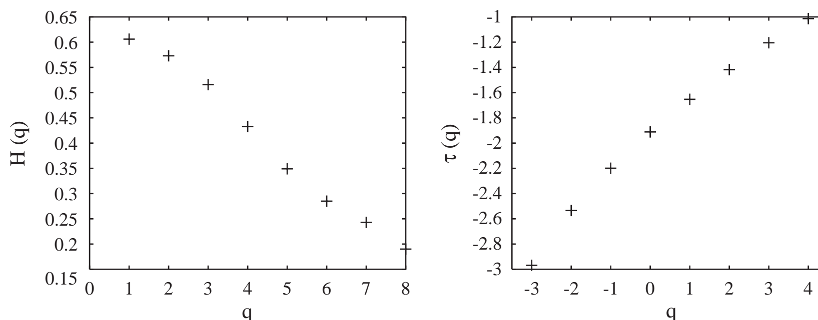

Fig. 9. $H(q)$ (left) and $\tau(q)$ (right) spectrum for real GaAs surfaces. The nonlinearity is a sign of multifractality.

the fractal properties of randomly rough surfaces evaluated using AFM.

The practical meaning of both of these theoretical analyses consists in the numerical evaluation of the tip influence on the fractal properties of surfaces that are estimated to be self-affine. The results of this analysis can enable us to perform a rough estimation of the errors achieved within AFM studies of these surfaces. Further, these results allow us to estimate the corrections of the fractal properties parameters mentioned above to be obtained using the correcting procedures (e.g. the procedure presented by Villarubia). It was unfortunately shown that the surface reconstruction procedure did not correct the results of the multifractal analysis of the randomly rough surfaces in a substantial way. Thus it is practically impossible to remove the influence of the AFM tip convolution at the multifractal analysis of the randomly rough surfaces. One can expect that this tip convolution affects the analysis of very fine randomly rough surfaces in particular. This means that the main result of the effort connected with this paper consists in the conclusion that it is impossible to correct the negative influence of the tip convolution on the fractal properties of the surfaces in a substantial way. This conclusion is very important from the practical point of view.

The theoretical results presented in this article were illustrated using the multifractal analysis of the randomly rough surfaces of GaAs single crystals prepared by means of their thermal oxidation. It should be noted that the rough surfaces of GaAs did not exhibit too fine roughness. One can expect that for finer surface roughnesses the effects of the tip convolution on the multifractal analysis investigated in this paper will be more pronounced.

Acknowledgements

This work was supported by the Grant Agency of the Czech Republic under contracts 101/01/1104 and 202/01/1110.

References

[1] C. Douketis, Z. Wang, T.L. Haslett, M. Moskovits, Phys. Rev. B 51 (1995) 16.
[2] A. Van Put, A. Vertes, D. Wegrzynek, B. Treiger, R. Van Grieken, Fresenius J. Anal. Chem. 350 (1994) 440.
[3] J. Krim, G. Palasantzas, Int. J. Mod. Phys. B 9 (1995) 599.
[4] J.M. Gómez-Rodríguez, L. Vázquez, A.M. Baró, Surf. Inter. Anal. 16 (1990) 97.
[5] W. Zahn, A. Zösch, Fresenius J. Anal. Chem. 365 (1999) 168.
[6] A. Mannelquist, N. Almqvist, S. Fredriksson, Appl. Phys. A 66 (1998) 891.
[7] A.-L. Barabási, R. Bourbonnais, M. Jensen, J. Kertész, T. Vicsek, Y.-Ch. Zhang, Phys. Rev. A 45 (1992) R6951.
[8] Z.R. Struzik, Fractals 8 (2000) 163.
[9] N. Scafetta, L. Griffin, B.J. West, Physica A 328 (2003) 561.
[10] A. Arnéodo, N. Decoster, S.G. Roux, Eur. Phys. J. B 15 (2000) 567.
[11] J.S. Villarubia, J. Res. Natl. Inst. Stand. Technol. 102 (1997) 425.
[12] T.H. Keitt, Landscape Ecol. 15 (2000) 479.